ANALYTICAL SCIENCES NOVEMBER 2016, VOL. 32

Notes

A Perturbation Analysis to Understand the Mechanism How Migrating Cells Sense and Respond to a Topography in the Extracellular Environment

Hiromi MIYOSHI,[*1,*2†] **Kensuke SUZUKI,**[*2,*3,*4] **Jungmyoung JU,**[*4] **Jong Soo KO,**[*5] **Taiji ADACHI,**[*3] **and Yutaka YAMAGATA**[*4]

*1 *Pathophysiological and Health Science Team, RIKEN Center for Life Science Technologies, 6-7-3 Minatojima-minamimachi, Chuo, Kobe, Hyogo 650–0047, Japan*
*2 *PRIME, AMED, 6-7-3 Minatojima-minamimachi, Chuo, Kobe, Hyogo 650–0047, Japan*
*3 *Laboratory of Biomechanics, Department of Biosystems Science, Institute for Frontier Life and Medical Sciences, Kyoto University, 53 Kawahara-cho, Shogoin, Sakyo, Kyoto 606–8507, Japan*
*4 *Ultrahigh Precision Optics Technology Team, RIKEN Center for Advanced Photonics, 2-1 Hirosawa, Wako, Saitama 351-0198, Japan*
*5 *Graduate School of Mechanical Engineering, Pusan National University, Jangjeon-dong, Geumjeong-gu, Busan 609-735, Korea*

Migrating cells *in vivo* monitor the physiological state of an organism by integrating the physical as well as chemical cues in the extracellular microenvironment, and alter the migration mode, in order to achieve their unique function. The clarification of the mechanism focusing on the topographical cues is important for basic biological research, and for biomedical engineering specifically to establish the design concept of tissue engineering scaffolds. The aim of this study is to understand how cells sense and respond to the complex topographical cues *in vivo* by exploring *in vitro* analyses to complex *in vivo* situations in order to simplify the issue. Since the intracellular mechanical events at subcellular scales and the way of the coordination of these events are supposed to change in the migrating cells, a key to success of the analysis is a mechanical point of view with a particular focus of the subcellular mechanical events. We designed an experimental platform to explore the mechanical requirements in a migrating fibroma cell responding to micro-grooves. The micro-grooved structure is a model of gap structures, typically seen in the microenvironments *in vivo*. In our experiment, the contributions of actomyosin force generation can be spatially divided and analyzed in the cell center and peripheral regions. The analysis specified that rapid leading edge protrusion, and the cell body translocation coordinated with the leading edge protrusion are required for the turning response at a micro-groove.

Keywords Cell migration, micro-groove, actomyosin force generation, adhesion complex

(Received June 28, 2016; Accepted August 25, 2016; Published November 10, 2016)

Introduction

Cell migration is a critical process in immune response, embryonic development, tissue formation, maintenance, and regeneration. In order to achieve these unique functions, migrating cells *in vivo* monitor the physiological state by integrating the extracellular environmental cues, and alter the migration mode.[1] Clarification of the mechanism is important for basic biological research and in biomedical engineering to establish the design concept of a tissue engineering scaffold.

Within the extracellular microenvironmental cues, the significance of the physical properties of the extracellular matrix (ECM), involving its topography, has been increasingly recognized.[2,3] The ECM topography varies, ranging from two-dimensional (2D) tight calcified collagen in bone and teeth, macroscopically 2D, but micrometer-/nanometer-scale porous basement membrane (*i.e.* 2.5 dimension at the cellular and subcellular scales), and a complex three-dimensional (3D) fibrillar collagen polymer network in connective tissues.[4] It is known that the cells can sense these topographical features and alter the mode of cell migration,[5] although the mechanism is still far from being clarified.

Our current understanding of the mechanism of cell migration is primarily derived from studies using a cell culture substrate with 2D rigid glass or plastic surfaces.[6] Recently, advanced 2D cell culture substrates with modifications of the chemical[7] and mechanical[8] properties at sub-cellular scales are given by micro-/nano-engineering techniques. Each of the conventional and advanced 2D substrates provides the cells with a wide continuous surface for exploration and migration. In contrast, most *in vivo* extracellular environments are 2.5D or 3D which is characterized by gaps (the porosity in the 3D environment). The gaps could significantly affect the exploratory and migratory behaviors of cells *in vivo*. Thus, understanding how cells sense and respond to the gap structures by the *in vitro* experimental system with a micro-/nano-structure accelerates to our

† To whom correspondence should be addressed.
E-mail: hiromi-miyoshi@riken.jp

understanding of cell migration in a complex environment *in vivo* by the extrapolation of *in vitro* analyses to *in vivo* situations.[9]

The subcellular mechanical events for cell migration are supposed to be altered due to the interaction of cells with the micro-/nano-topographies.[5] The key subcellular mechanical events involve membrane protrusion by actin polymerization, formation of the adhesion complex that links the extracellular environment and the endogenous actin cytoskeleton, as well as retraction at the rear by the contractile forces, resulting from the actin-myosin interaction. The mode of cell migration is changed by the changes in these subcellular events, and further by how to coordinate these events.[1] Thus, a key to the success of analysis to understand the mechanism of how migrating cells sense and respond to the micro-topographical cues is a mechanical point of view with particular consideration of the subcellular events for cell migration.

We designed an experimental platform to clarify the mechanical requirements for the cell migratory response to a topographical cue, specifically gap structures. To simplify the issue, a single microgroove, which is thought to be a geometrically simple gap structure, was adopted as the topographical cue. The analysis was based on observations of the gerbil fibroma cells and those treated with two types of inhibitors, Y-27632 and ML-7, both of which affect the endogenous actomyosin force generation through the inhibition of myosin phosphorylation, but have different target molecules. Y-27632 is known to be an inhibitor of Rho-associated protein kinase (ROCK). Since ROCK regulates myosin phosphorylation in a cell center region,[10,11] Y-27632 disturbs the myosin phosphorylation mainly in the cell center region. ML-7 is known as an inhibitor of myosin light chain kinase (MLCK). Since MLCK regulates myosin phosphorylation in a cell peripheral region,[10,11] ML-7 disturbs the myosin phosphorylation mainly in the cell peripheral region. Thus, by using Y-27632 and ML-7, the contributions of the subcellular mechanical events, which are actomyosin force generation in the cell center and that in the cell peripheral regions, to sensing and responding to micro-topographical cues, can be spatially divided and analyzed.

Experimental

PDMS substrate fabrication

We fabricated a polydimethylsiloxane (PDMS) test substrate with line grooves. The width of each groove was 20, 10, or 3.5 μm. The depth of the grooves was fixed to be 10 μm. The PDMS substrate was made by replication of the mold with rectangular ridges of epoxy resin (SU-8) on a silicon wafer. The PDMS substrates were treated with oxygen plasma for 1 min to make the surface to increase hydrophilicity, and coated with fibronectin (20 μg/ml) for 1 h.

Live cell microscopy and the analysis of IMR33 gerbil fibroma cell migration

IMR 33 gerbil fibroma cells were purchased from ATCC and cultured in Medium199 (Sigma) containing fetal bovine serum (Sigma) and penicillin-streptomycin (100 units/mL penicillin, and 100 μg/mL, Sigma). The cells were plated on a 20 μg/ml fibronectin coated PDMS substrate, and incubated at 37°C overnight. Then, time-lapse phase contrast images were acquired using an inverted microscope (IX83-ZDC, Olympus) with a 10× 0.3NA UPlanFLN objective lens (Olympus). An iXonEM EMCCD camera (DU897, Andor Technology) captured digital greyscale images every 2 min.

The response of cells encountering a groove was classified into three types: (1) "Turn type" was defined for the cells that turned at the groove within 3 h after the leading edge initially contacted with the edge of the groove; (2) "Constraint type" was defined for the cells that kept contact with the groove for over 3 h; (3) "Cross type" was defined for the cells that crossed the groove within 3 h.

Perturbation of the actomyosin force generation in a cellular region specific manner

For perturbation of the actomyosin force generation in the cellular region specific manner, 10 μM Y-27632 (Sigma) or 50 μM ML-7 (Sigma) was used. These reagents disturb myosin phosphorylation in different regions.[10,11]

The effects were checked by fluorescent staining performed by fixing cells in 4% paraformaldehyde for 15 min. Cells were washed and permeabilized with 0.2% Triton-X, and blocked with 0.2% gelatin in PBS. After several washes, the cells were incubated with a first antibody (anti-vinculin Mouse IgG, Sigma; or anti-Talin Mouse IgG, Gene Tex) for 1 h, and then with alexa546 labeled anti-mouse IgG for 1 h. For filamentous actin staining, the fixed and immunofluorescence stained cells were incubated with Alexa Fluor488 phalloidin (diluted 1:40, Invitrogen) for 1 h. The fixation and staining were all carried out at room temperature. Fluorescent images were acquired using a confocal laser scanning microscope (FV1200 IX83, Olympus) with a 60× 1.2NA UPlanSApo water immersion objective lens (Olympus).

Results and Discussion

Migratory behavior of IMR 33 gerbil fibroma cells at microgrooves

First, we observed the migratory behaviors of IMR33 cells at the grooves with 20, 10, and 3.5 μm in width and constant 20 μm in depth.

At the 20 μm-groove, the cells never migrated down to the groove, but exhibited turn-type and constraint-type migrations. Typical turn-type migration at the 20 μm-groove was, as shown in Fig. 1a, that the cells migrating toward the groove (arrow head, 0 – 30 min) retracted the lamella at the edge of the groove, and changed the direction of the lamellar extension (30 – 60 min), followed by a change in their migratory direction (90 min). In constraint-type migration at the 20 μm-groove, as shown in Figs. 1b and 1c, two typical cases were observed. One constraint type was, as shown in the cell indicated by the arrowhead in Fig. 1b, that the cells moved along the edge of the groove for over 3 h. The other was, as shown in the cell indicated by the arrowhead in Fig. 1c, that the cells stopped at the edge of the groove with a bipolar shape for over 3 h. The migratory behavior of an identical cell repeatedly encountering the 20 μm-groove was different in each event, *i.e.*, sometimes the turn type, and at other times the constraint type. At a narrower groove with 10 μm in width, IMR33 cells showed the turn type or the constraint type in a similar manner to those at the groove with 20 μm in width.

On the other hand, IMR33 cells encountering a further narrower groove with 3.5 μm in width showed the cross type. In typical cross-type migration, as shown in Fig. 1d, lamella extended over the groove, and then the cell body crossed over the groove (30 – 60 min). Not only the cross type, but also turn type and constraint type were observed at the 3.5 μm-groove. However, both in the turn type and constraint type, the details

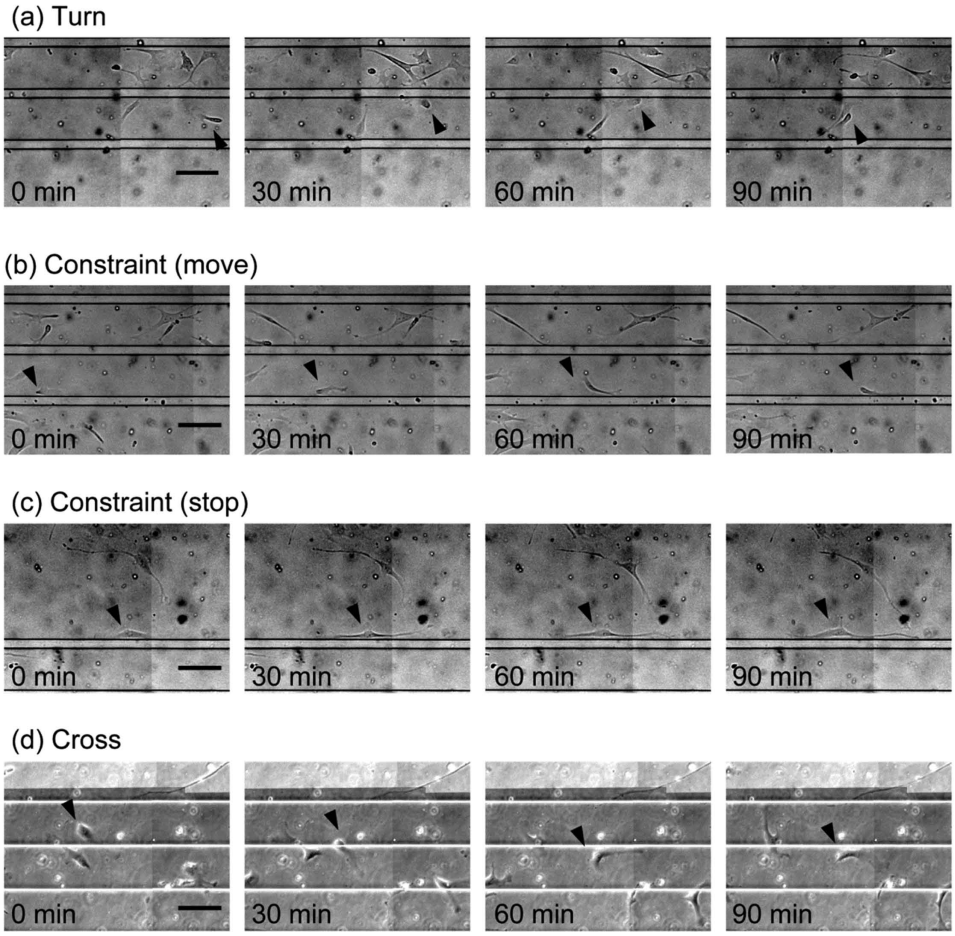

Fig. 1 Phase contrast micrographs showing typical migratory behaviors of IMR 33 cells. (a, b, c) Turn type (a) and constraint types (b, c) at a 20 μm-groove. (d) Cross type at a 3.5 μm-groove. Scale bars, 100 μm.

on the migratory behavior were different from those at the 10 and 20 μm-grooves. Lamella transiently crossed over the narrow 3.5-μm groove (the cell indicated by the arrowhead at 180 min in Fig. S1 for the turn type; the cell indicated by the arrowhead from 120 to 180 min in Fig. S2 for the constraint type), whereas the lamella never crossed over the 20 and 10 μm-grooves.

In Fig. 2a, the frequency of the migratory patterns of IMR33 cells at the 20, 10, and 3.5 μm-grooves are summarized. The graph clearly shows that the turn type decreased and the cross type increased as the groove width decreased. This would be due to an increase in the probability of lamella crossing over the groove, since the lamella transiently crossed over the 3.5-μm groove, even in the cross type and the constraint type. The result indicates that the IMR 33 cells have an ability to detect the width of the groove and change their migratory pattern depending on the groove width.

Perturbation of spatial regulation of endogenous mechanical force generation and its effect on cell migratory behavior at the microgrooves

To consider the mechanism in IMR33 cells to sense the groove width and to determine their migratory behavior from the mechanical point of view, we treated the cells with Y-27632 or ML-7, and did the same observations as that for the untreated cells. As shown in Figs. 2b and 2c, the turn-type migratory responses at the 10 and 20 μm-grooves were impaired and altered by a constraint type. On the other hand, the migratory behaviors at the 3.5 μm-groove remained to be unchanged both by the Y-27632 treatment and by the ML-7 treatment. These results suggested that actomyosin force generation both in the cell center region and the peripheral region is required for the turn-type response of IMR33 cells at the 10 and 20 μm-groove. To explore the intracellular factors contributing to the turning response, we observed the change in the cellular distributions of immature and mature adhesions, and actin network in untreated, Y-27632, and ML-7 treated IMR33 cells.

In untreated IMR33 cells immature adhesions, which can be detected by talin accumulation, were continuously distributed in the periphery of the leading lamella (Fig. 3a). Matured adhesion spots, which can be detected by vinculin accumulation, were distributed all over the ventral cell surface, as shown in Fig. 3b. The filamentous actin was well oriented normal to the leading edge in the leading lamella (Fig. 3c).

Y-27632 is known to disturb myosin phosphorylation in the center region of cells.[10] Consistently, actin stress fibers were disappeared from the cell center region in the Y-27632 treated cells (Fig. 3f). It is known that the maturation of cell adhesions requires a mechanical force generated by the actomyosin interaction.[12] Thus, as predicted, the Y-27632 treatment also led to the disappearance of matured adhesion spots with vinculins in the inner lamella and the cell body, *i.e.* cell center region, as shown in Fig. 3e.

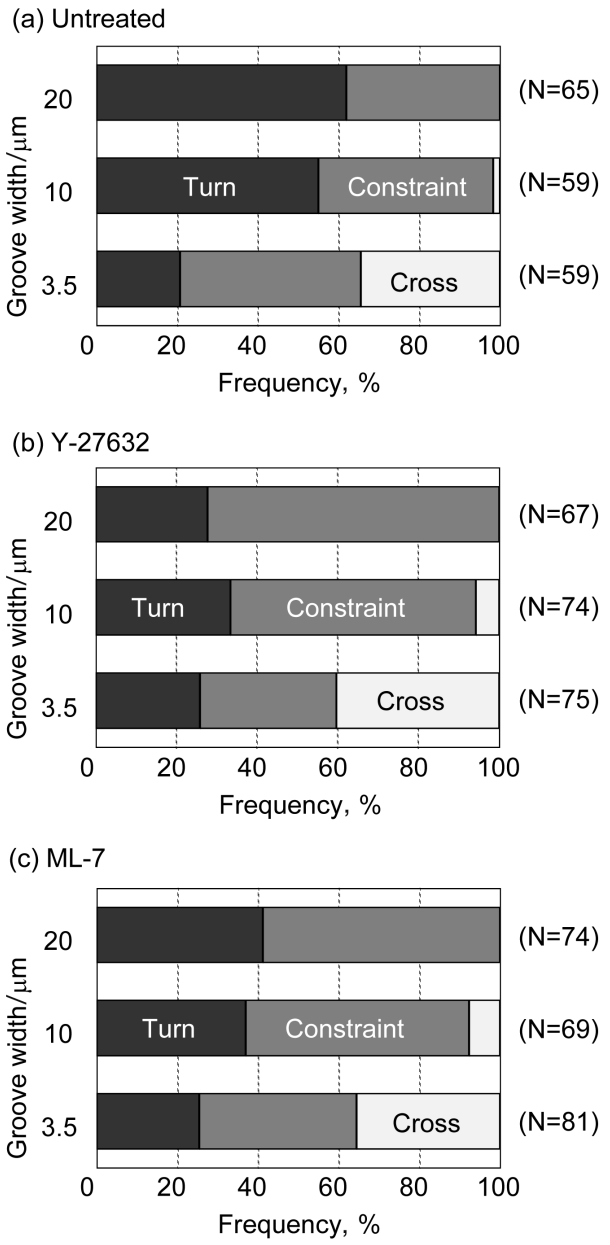

Fig. 2 Frequency of the migration patterns of IMR 33 cells at the 20, 10, and 3.5 μm-groove. The results for (a) inhibitor untreated, (b) Y-27632 treated, and (c) ML-7 treated cells. The numbers of cells observed are shown in right-hand side of each bar.

MLCK is known to mainly regulate myosin phosphorylation throughout the lamella from the leading edge to the base of the cell body,[10,11] thus, the MLCK inhibitor ML-7 will affect the myosin phosphorylation throughout the lamella. In the ML-7 treated cells, as shown in Fig. 3g, immature adhesions, which were detected by talin accumulation, remained in the leading lamella. The talin distribution in the ML-7 treated cells showed the same result as that in the untreated cells. On the other hand, the matured adhesion spots disappeared from the ventral cell membrane throughout the lamella. These results are consistent with the previous finding that the mechanical force by the actomyosin interaction would not be necessary for talin accumulation to the immature adhesions, but would be closely related to vinculin accumulation to the matured adhesion spot.[13,14] Concerning the distribution of the actin filaments in the leading lamella, their orientation normal to the leading edge was disrupted (Fig. 3i).

Hypothesized mechanical requirements for the turning behavior at microgrooves

Based on these results concerning an analysis of the cell migratory response and the cellular distributions of adhesion proteins and actin cytoskeleton, we hypothesize the mechanical requirements in IMR33 cells of the turning response at the 10 and 20 μm-grooves of which size was the same order as a whole cell.

Our observation (Fig. 1a) demonstrated that turning IMR33 cells rapidly retracted the leading lamella, and changed the direction of lamellar extension, followed by a change in the moving direction of the cell body. In these cells, the matured adhesion spots including vinculins in the inner lamella and the cell body work as the point of force application by actin stress fibers, and contribute to the traction of the cell body and retraction of the trailing edge.[15] Our hypothesis is that the inhibition of actomyosin force generations in the cell center region by Y-27632 disrupts the force application points, which slows the cell body translocation that follows the lamella extension. The perturbation of the cell body translocation leads to decrease the turning response of the cell. Our analysis showed that the effect of ML-7 was also to decrease the turning response, although the target of ML-7 is not the cell center region, but the cell periphery. The ML-7 treatment is assumed to impair another requisite for IMR33 cells to turn at 10 and 20 μm-groove, *i.e.* rapid retraction of the leading lamella. Specifically, the inhibition of actomyosin force generation in the cell peripheral region by ML-7 disrupts the orientation of the contractile actin filaments normal to the leading edge, as well as the matured adhesion spots including vinculins that work as the anchorage points of the contractile actin filaments. These effects will lower the activities of the leading edge retraction at the 10 and 20 μm-grooves, and decrease the turning response of the IMR33 cells.

Conclusions

Our analysis enabled us to specify the two mechanical requirements for the cell turning response to a cellular-sized microgroove. One is a rapid retraction of the leading lamella, which results from the actomyosin network that orients normal to the leading edge with the anchoring point consisting of matured adhesion spots in the cell peripheral region. The other is the cell body translocation well-coordinated with the rapid lamella extension, which results from actin stress fibers with the force application points consisting of the matured adhesion spots in the cell center region. The expansion of the findings regarding the gap sensing and the migratory response in the gerbil fibroma cell into other types of topography with different sizes and the other types of cells will lead to acquire a higher degree of generalized insight into the mechanism of how migrating cells *in vivo* sense and respond to the topography of the extracellular environment.

Acknowledgements

This work was partially supported by PRIME, AMED, and a Grant for Facilitation of Innovation Processes from RIKEN Baton Zone Programs Office. We also thanks the RIKEN BOCC for confocal microscopy.

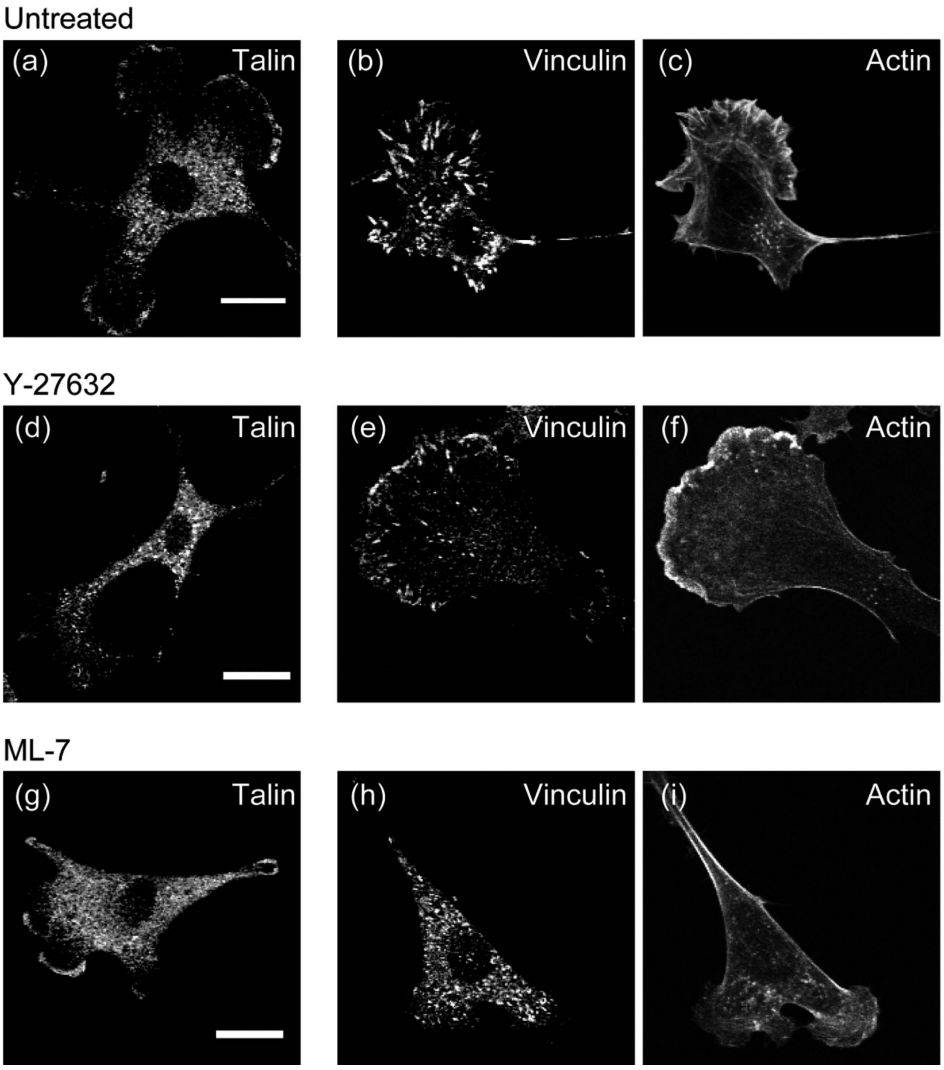

Fig. 3 Typical distributions of immature and mature adhesions and actin filaments in IMR33 cells. The fluorescent micrographs of talin staining (a, d, g), and double staining vinculin (b, e, h) and actin filaments (c, f, i) in untreated (a, b, c), Y-27632 treated (d, e, f), and ML-7 treated cells (g, h, i). Scale bars, 20 μm.

Supporting Information

Figures S1 and S2 are available free of charge on the Web at http://www.jsac.or.jp/analsci/.

References

1. P. Friedl and K. Wolf, *J. Cell Biol.*, **2010**, *188*, 11.
2. M. P. Lutolf and J. A. Hubbell, *Nat. Biotechnol.*, **2005**, *23*, 47.
3. N. A. Kurniawan, P. K. Chaudhuri, and C. T. Lim, *J. Biomech.*, **2016**, *49*, 1355.
4. K. Wolf and P. Friedl, *Trends Cell Biol.*, **2011**, *21*, 736.
5. H. Miyoshi and T. Adachi, *Tissue Eng. Part B*, **2014**, *20*, 609.
6. A. D. Doyle and K. M. Yamada, *Exp. Cell Res.*, **2016**, *343*, 60.
7. J. Nakanishi, *Chem.—Asian J.*, **2014**, *9*, 406.
8. A. Ueki and S. Kidoaki, *Biomaterials*, **2015**, *41*, 45.
9. G. Charras and E. Sahai, *Nat. Rev. Mol. Cell Biol.*, **2014**, *15*, 813.
10. G. Totsukawa, Y. Wu, Y. Sasaki, D. J. Hartshorne, Y. Yamakita, S. Yamashiro, and F. Matsumura, *J. Cell Biol.*, **2004**, *164*, 427.
11. G. Totsukawa, Y. Yamakita, S. Yamashiro, D. J. Hartshorne, Y. Sasaki, and F. Matsumura, *J. Cell Biol.*, **2000**, *150*, 797.
12. M. L. Gardel, I. C. Schneider, Y. Aratyn-Schaus, and C. M. Waterman, *Ann. Rev. Cell Dev. Biol.*, **2010**, *26*, 315.
13. A. del Rio, R. Perez-Jimenez, R. C. Liu, P. Roca-Cusachs, J. M. Fernandez, and M. P. Sheetz, *Science*, **2009**, *323*, 638.
14. R. Janostiak, A. C. Pataki, J. Brabek, and D. Rosel, *Eur. J. Cell Biol.*, **2014**, *93*, 445.
15. T. Vallenius, *Open Biol.*, **2013**, *3*, 130001.